
Collision-induced Dissociation Mass Spectrometry of Nonionic Surfactants Following Direct Supercritical Fluid Injection

Henry T. Kalinoski and Leonard O. Hargiss

Unilever Research U.S., Edgewater, New Jersey, USA

Direct injection from a capillary supercritical fluid chromatography system was used as an inlet technique for chemical ionization (CI) and low energy collision-induced dissociation (CID) mass spectrometry of a series of low volatility nonionic surfactant mixtures. Characteristic fragment ions produced by CID for various classes of nonionic surfactant molecules were found to depend greatly on the structure of the surfactant hydrophobe. This was the case even when the charge on the molecule appeared localized away from the hydrophobe. Numerous decomposition pathways are suggested by the fragment ions produced. The use of direct supercritical fluid injection as an inlet technique does not appear to influence adversely the ability to produce CID mass spectra. Direct supercritical fluid introduction allows CI to be compared with other ionization mechanisms more commonly used for multifunctional, low volatility samples. (*J Am Soc Mass Spectrom* 1992, 3, 150-158)

Characterization of complex mixtures of low volatility oligomeric materials has been facilitated through advances in supercritical fluid separation techniques and the direct interface of supercritical fluid chromatography (SFC) with mass spectrometry (SFC/MS) [1-7]. Molecular weight and fragmentation information available from mass spectrometry complements the fast, efficient separations attainable with capillary SFC. Other advantages of the capillary direct SFC/MS interface, at least as compared with liquid chromatography/MS, include simple direct interfacing for "traditional" chemical ionization (CI) and ease of mobile phase removal.

One compound class particularly amenable to SFC and SFC/MS characterization is the nonionic surfactants, the second largest class of synthetic detergents. Over 800 million pounds of nonionics are consumed annually in the United States, the majority in household detergent products. Nonionic surfactants are often used in combination with other detergents, usually anionics, to modify properties of consumer cleaning products. Commercial nonionic surfactant mixtures are comprised of an ethoxylated or propoxylated hydrophile (repeating ethylene or propylene ethers), a terminal end group (often, but not necessarily, a hydroxyl group), and an alkyl or alkyl-substituted aryl hydrophobe. The hydrophobe may be straight or branched, may be unsaturated, or may

contain reactive functionalities. Substituted aryl hydrophobes may be mixtures of numerous isomers. Structural variations determine physical properties, influence biodegradability, and affect chromatographic behavior. Commercial surfactant mixtures often also contain many minor components related to side products of synthetic reactions used to produce the principal components. Characterization requires information on the structure(s) of the hydrophobe, hydrophobe chain-length distribution, type, length, and distribution of hydrophile and identification of terminal groups.

Conditions have been determined which optimize parent ion production for nonionic surfactants in SFC/MS and have been used to obtain average molecular weights and hydrophile distributions for surfactant mixtures [3]. Conditions optimal for producing molecular weight information, however, limit the type and amount of structural information available regarding mixture components. To increase the amount of structural information available, capillary SFC has now been coupled with tandem mass spectrometry (MS/MS). The goal was to extend work on SFC/MS of surfactants [1, 3] and on collision-induced dissociation (CID) of polyglycols [8] to address questions of characterization of low molecular weight, substituted oligomeric materials. Direct capillary supercritical fluid introduction allows the use of "traditional" CI with somewhat polar, less volatile species without the use of high temperatures for sample vaporization. CI provides a more well-defined, controllable ionization than

Address reprint requests to Henry T. Kalinoski, Unilever Research U.S., 45 River Road, Edgewater, NJ 07020.

the method more typically used for such samples, namely fast-atom bombardment (FAB).

A capillary SFC system interfaced with CI MS/MS was applied to a variety of polyethoxylated and polypropoxylated samples to determine if characteristic fragment ions could be produced. The results were compared with those of an FAB/MS/MS study of related materials [8], which had indicated very little fragmentation was found for cationized polyalkoxylates in low energy CID. Results of the present work indicated low energy CID spectra of CI-generated surfactant ions, produced on a tandem quadrupole instrument, are influenced by the type of hydrophobe present. Ions diagnostic of hydrophobe type are produced in SFC/MS/MS and structural information for some hydrophobe types is available. The mobile phase used for supercritical fluid introduction does not interfere with CID studies and can be used as the CI reagent for additional information or flexibility. A variety of mechanisms, dependent on hydrophobe type and structure, appear responsible for the CID fragment ions produced.

Experimental

All experiments were performed on a Finnigan-MAT TSQ-70B tandem quadrupole mass spectrometer (Finnigan-MAT, San Jose, CA). The combination electron ionization-CI ion source with the chromatography-CI ion volume was used. Ion source temperature was 150 °C for all experiments. Methane, isobutane, ammonia, and dichlorodifluoromethane (Freon-12) (AGL, Clifton, NJ) of the highest available purity were used as CI reagents. A mixture of 7.7 mol % 2-propanol (Fisher Scientific, Co., Fair Lawn, NJ) in carbon dioxide, prepared for use as chromatographic mobile phase, was also used as CI reagent. Reagent gas pressure required for CI varied from 0.2 (CO₂/propanol) to 7 torr (ammonia) as measured using a Pirani gauge on the reagent gas inlet line. Reagent gas pressures were optimized for maximum parent ion production. No effort was made to maintain constant ion volume pressure or reagent gas/mobile phase ratio. CID was performed using argon collision gas at a cell pressure of 1.6 mtorr. Collision energy was either set prior to sample introduction (20-100 eV) or incrementally increased on successive scans during elution of the species of interest using an instrument control language procedure described by Lammert [9]. The latter approach allowed for rapid screening of collision energy to optimize CID conditions for maximum daughter ion yield. Mass scan range depended on the sample being analyzed, usually at a rate of 500 u/s. Both quadrupoles 1 and 3 were tuned and calibrated to 1500 u by using perfluorononyl-s-triazine (PCR, Inc., Gainesville, FL) and operated at unit mass resolution through this range.

A Lee Scientific model 602 SFC (Lee Scientific, Salt Lake City, UT) was used for minimal chromatographic

separation (to separate sample from solvent) and direct injection sample introduction. A 1-m length of 50- μ m i.d. fused silica open tubular column with a 50% octyl methylpolysiloxane stationary phase (SB-Octyl-50, Lee Scientific) was used for limited resolution separation. Separations were conducted at 125 °C with a 140 bar/min pressure ramp from 100 to 400 bar followed by a hold at 400 bar until completion of the experiment, primarily to separate sample from solvent. A porous ceramic "frit" restrictor (Lee Scientific) was used to maintain column pressure. The Finnigan capillary-direct interface was maintained at 125 °C, with the restrictor heater held at 250 °C.

Carbon dioxide, 7.7 mol % 2-propanol in carbon dioxide and Freon-12 were used as supercritical mobile phases. The 2-propanol in carbon dioxide mixture was prepared by weighing approximately 30 g of propanol into an evacuated aluminum lecture bottle (size F cylinder, Scott Specialty Gases, Plumsteadville, PA) cooling, and filling the cylinder with carbon dioxide. The exact amount of CO₂ (~270 g) was calculated by subtracting the cylinder tare weight and weight of alcohol from the weight of the full cylinder. Care should be taken not to overfill the cylinder and risk overpressurization. Contents of the cylinder were mixed using a Teflon-coated stirring bar and magnetic stirrer. The cylinder was inverted to fill the syringe pump.

Solutions of alkoxyated nonionic surfactant samples (Table 1) were prepared in dichloromethane (Optima grade, Fisher Scientific) at concentrations of 50 mg/mL. Samples were obtained from various sources (as indicated) and used as received. A 0.5- μ L sample was injected using the helium-actuated microinjector (model 7526, Rheodyne, Cotati, CA) and flow-split using an approximate split ratio of 50:1. Representative structures of surfactants are given in Table 1. One limitation in the work was that many samples were mixtures for which complete structural information on components was unavailable. In Table 1 these samples are marked * and structures given should not be taken to be exact representations of known configurations.

Results and Discussion

Figure 1 shows the argon CID mass spectrum of the ammonium adduct ion of octa(ethylene glycol) methyl ether following CO₂/propanol SFC and ammonia positive chemical ionization (PCI). For simple polyethylene glycols (PEGs) and their monomethyl ethers, low energy CID results found following SFC/CI were comparable to those previously reported for FAB ionization [8]. Only the presence of two ion series, one hydroxy terminated and one terminated by the methyl ether, distinguish the spectrum in Figure 1 from CID spectra of PEG molecules. Similar results were obtained from protonated PEG-methyl ether molecules formed using isobutane or propanol PCI. For both

Table 1. Nonionic Surfactants Used

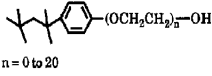
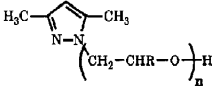
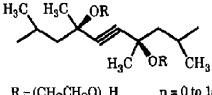
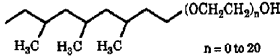
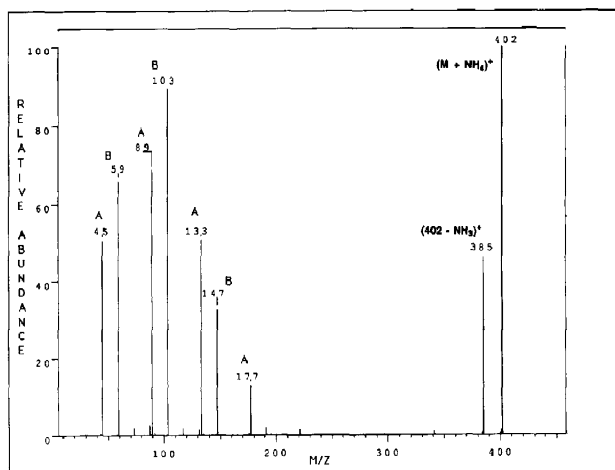
Sample	Supplier	Hydrophobe Type	General Structure
Polyethylene Glycol	Aldrich	none	$\text{HO}(\text{CH}_2\text{CH}_2\text{O})_n\text{H}$
Polyethylene Glycol Monomethyl Ether	Aldrich	none	$\text{HO}(\text{CH}_2\text{CH}_2\text{O})_n\text{CH}_3$
Tetradecanol Hexaethoxylate	Nikko	linear primary alcohol	$\text{CH}_3(\text{CH}_2)_{12}\text{CH}_2\text{O}(\text{CH}_2\text{CH}_2\text{O})_6\text{H}$ $m = 12, n = 6$
Hexadecanol Hexaethoxylate	Nikko	linear primary alcohol	$m = 14, n = 6$
Alfonic 1412:70	Conoco	linear primary alcohol	$m = 10 \text{ or } 12, n = 0 \text{ to } 20$
Triton X-165	Rohm and Haas	alkylphenol	 $n = 0 \text{ to } 20$
Tergitol 15-S-12	Union Carbide	secondary alcohol*	$\text{H}_3\text{C}-\text{CH}-(\text{CH}_2)_m-\text{CH}_3$ $(\text{OCH}_2\text{CH}_2)_n-\text{OH}$ $m = 8 \text{ to } 12, n = 0 \text{ to } 20$
OXYPRUF "E" and "P"	Olin Chemical	pyrazole	 $\text{R} = \text{H or CH}_3, n = 1 \text{ to } 20$
Surfynol 465	Air Products and Chemical	tetramethyldecyne diol*	 $\text{R} = (\text{CH}_2\text{CH}_2\text{O})_n\text{H} \quad n = 0 \text{ to } 15$
Tergitol TMN6	Union Carbide	trimethylnonyl alcohol*	 $n = 0 \text{ to } 20$

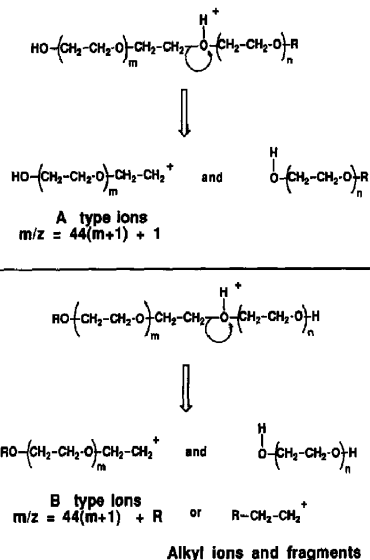
Figure 1. The 40-eV (lab) argon CID mass spectrum of the ammonium adduct ion (MHN_4^+) of octa(ethylene glycol) methyl ether, $m/z = 402$. The poly(ethylene glycol) methyl ether mixture was separated using a carbon dioxide/2-propanol supercritical mobile phase, as described in Experimental. Ammonia was used as reagent gas (7 torr) for positive chemical ionization. Fragment ions labeled A and B are believed to be of the structure given in Scheme 1. Similar fragment ions were found in CID of protonated molecules (MH^+).



PEG and PEG-methyl ether samples, the charge site-initiated decomposition previously described [8] and shown in Scheme I accounts for the fragment ions produced, whether the (MH^+) or $(M + NH_4^+)$ ions are analyzed. These same types of ions have been observed in high energy CID of poly(ethylene glycols) [10]. Series A ions ($m/z = 45, 89, 133, 177,$ etc.) arise from the hydroxy terminus and the related B series carry the methyl ether terminus ($m/z = 59, 103, 147, 191,$ etc.). Not found, for the range of collision energies studied here (20–100 eV, lab), were ions corresponding to the loss of 44 u, CH_2CH_2O , as seen in high energy CID of protonated PEG molecules following FAB [11, 12].

The CID mass spectrum of the ammonium adduct ion in Figure 1 differs from spectra of the protonated molecule of the same species by the ion due to the loss of ammonia (17 u) at $m/z = 385$. The proton and charge remain with the alkoxyated molecule. This reflects the high proton affinity for ethoxylated molecules reported by Lin et al. [13] in their work with ethoxylated linear primary alcohols.

Figure 2 shows the 60-eV (lab) argon CID mass spectrum of the protonated molecule of tetradecanol hexaethoxylate, $m/z = 479$, a linear, primary alcohol ethoxylate. Fragmentation of the ethoxylate chain to give the A ($m/z = 45, 89, 133, 177, 221, 265$) and B ($m/z = 241, 285,$ and 329) series ions accounts for a majority of the daughter ion current produced. An ion corresponding to the $C_{14}H_{29}^+$ alkyl ion ($m/z = 197$) and alkyl chain fragmentation (all alkyl fragment ions from $m/z 43$ to $m/z 141$) are also seen. Such fragmentation is potentially useful for characterizing surfactant hydrophobes. Protonation on the oxygen attached to the alkyl chain and charge-induced simple cleavage leads to the alkyl ion and smaller fragments. Alkyl fragmentation here is greater than was reported



Scheme I. Mechanism for the charge site-initiated decomposition of protonated molecules of poly(ethylene glycol) and poly(ethylene glycol) methyl ether following the route proposed by Lattimer et al. [8]. A similar pathway may be followed by alcohol ethoxylates, where the methyl group on the B ions would be replaced with the surfactant hydrophobe.

for similar samples with CID following FAB ionization [14]. This reference does not state the type of instrument used or specific CID energy used so distinctions may be due to instrumental and collision energy differences. However, distinctions between CI and FAB ionization prior to low energy collisional activation

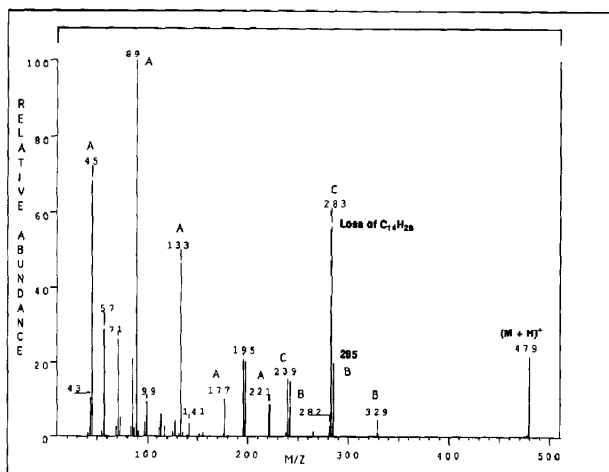


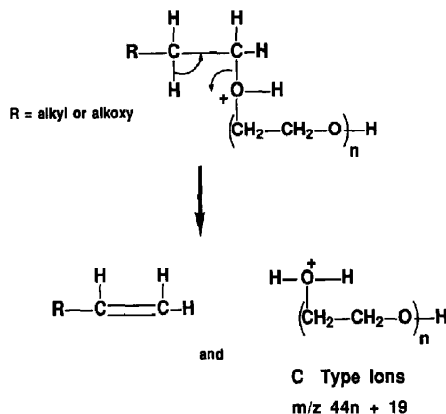
Figure 2. The 60-eV argon CID mass spectrum of the protonated molecule (MH^+) of tetradecanol hexaethoxylate, $m/z = 479$. A homogeneous sample of this material was introduced for isobutane (3 torr) PCI using supercritical CO_2 . A series ions are of the structure in Scheme I. B series ions have an R group of $C_{14}H_{29}$ with one ($m/z = 241$), two ($m/z = 285$), and three ($m/z = 329$) ethylene oxide units. Relative abundances of ions from $m/z = 190$ to $m/z = 470$ have been multiplied by a factor of 15. The fragment ion mass range was scanned from 20 to 500 u.

have been documented to affect overall fragmentation patterns [15] and work is underway to clarify this point.

The ion series labeled C ($m/z = 195, 239, 283$) in Figure 2 appears to be due to loss of the hydrophobe as an alkene (196 u, $C_{14}H_{28}$). This type of loss is not explained by the mechanism described in Scheme I, but could be due to ether cleavage with hydrogen transfer as shown in Scheme II. This is a charge site-initiated mechanism leading to protonated PEG molecules and would not be unexpected under the low energy CID conditions used. A similar mechanism was described to explain fragmentation under high energy CID conditions [10]. This type of ion is of relatively low abundance for the linear, primary alcohol ethoxylates. Protonation at ether oxygens at or near the hydrophobe favors ion formation through the mechanism detailed in Scheme II, yielding fragment ions with six, five, and four ethylene oxide units. The decomposition shown in Scheme I appears to be favored by protonation at ether oxygens nearer the hydroxy terminal of the molecule. Loss of the hydrophobe as the alkene is desirable for characterizing surfactant molecules. Information on both mass of the hydrophobe and length of the alkoxy chain is available through this one fragmentation.

Not found under the conditions used were ions due to loss of 44 u (C_2H_4O) as seen in CID spectra following self-CI of linear alcohol ethoxylates produced on a Fourier transform mass spectrometric instrument [13]. No clear explanation of this difference is readily apparent, although kinetic effects likely play a strong role. Work with other ionization methods and collision energies may clarify this point.

Although the mass spectrum in Figure 2 was produced from an homogeneous, single chain length ethoxylate sample, the same results were obtained for

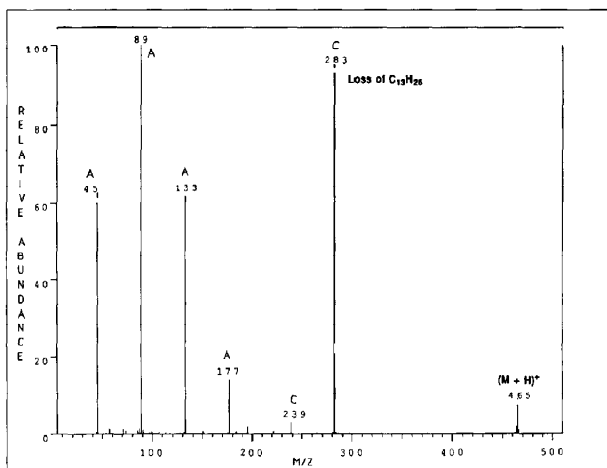


Scheme II. Mechanism to explain fragment ions corresponding to protonated poly(ethylene glycol) molecules, C, $m/z = 44n + 19$, found in CID mass spectra of nonionic surfactant materials. Protonation on the ether oxygen adjacent to the surfactant hydrophobe results in loss of the hydrophobe as a terminal alkene. Protonation in this charge site-initiated decomposition may occur at any of the oxygens along the alkoxy chain.

individual components of commercial mixtures of linear, primary alcohol ethoxylates (Alfonic 1412:70, Table 1).

Unfortunately, from the standpoint of structural characterization, the abundant end group fragmentation found for linear, primary alcohol ethoxylates was not found for other hydrophobe types. Figure 3 shows the 40-eV (lab) argon CID mass spectrum of the protonated molecule of secondary tridecanol hexaethoxylate ($m/z = 465$, from Tergitol 15-S-12, Table 1). Capillary SFC was conducted with a CO_2 /propanol mobile

Figure 3. The 40-eV argon CID mass spectrum of the protonated molecule of *sec*-tridecanol hexaethoxylate, $m/z = 465$, from Tergitol 15-S-12. This commercial secondary alcohol ethoxylate mixture was separated using a CO_2 /propanol supercritical mobile phase prior to isobutane (3 torr) PCI. The fragment ion mass range was scanned from 15 to 500 u.



phase and isobutane was used as CI reagent. The actual structure of the hydrophobe (position of alkoxylate substitution and possible chain branching) for this sample mixture is unknown and an original intention of this work was to investigate SFC/CI/MS/MS as a means of structural characterization of such materials. Decomposition of secondary alcohol ethoxylate ions is characterized by a dominant alkene loss ion ($m/z = 283$) and A series ions. No B type ions or fragments of the hydrophobe are produced. Even other C type ions ($m/z = 239, 195$) are of relatively low abundance. This might be evidence for primary protonation at the ether oxygen adjacent to the hydrophobe. Characteristics of the CID spectrum could help distinguish a linear, primary alcohol ethoxylate from a secondary alcohol surfactant, but are not very informative on structural features of secondary alcohol materials. The loss of alkene appears more facile for secondary alcohol surfactants, producing a more abundant fragment ion at lower collision energies (40 versus 60 eV) than were required for linear, primary alcohol ethoxylate materials.

As with secondary alcohol ethoxylates, structural information is desirable for characterizing branched alcohol surfactants. Figure 4 shows the 40-eV (lab) argon CID mass spectrum of the protonated molecule of a C_{12} branched nonaethoxylate (Tergitol TMN-6, Table 1), $m/z = 583$. The actual structure of the trimethylnonyl hydrophobe (sites of chain-branching) is uncertain. Carbon dioxide was used as the supercritical mobile phase and isobutane was used to produce positive CI mass spectra. Alkene loss and A series fragment ions dominate the spectrum, as was found with secondary alcohol materials. No alkyl fragment ions or B ions are produced. Loss of the alkene aids in determining hydrophobe and hydrophile chain lengths, but gives no information on the structure of the hydrophobe.

The type of hydrophobe present appears to have a strong effect on CID fragmentation of alcohol ethoxylates. Length of the hydrophile chain appears to exhibit little influence on fragmentation found. Homologues with hydrophile chain lengths from $n = 2$ to $n = 10$ were analyzed. Similar fragments (ion type and ion chain length) were found from long (seven or more alkylene oxide units) and short (three or fewer units) hydrophile chains. Protonation near the ether oxygen at the hydrophobe favors loss of the hydrophobe as the alkene (as illustrated in Scheme II). This does not conflict with the hydrogen-bound ring structure postulated for protonated alcohol ethoxylate molecules [13]. The cyclic structure explains formation of small polyethoxylate ions (m/z 45, 89, 133) but does not appear to account for facile loss of alkene. It is likely that all protonatable sites are protonated to some extent in a collection of parent ions and multiple pathways account for fragment ions observed.

Additional functionality on the hydrophobe results in formation of additional types of fragment ions. Figure 5 shows the 40-eV (lab) CID mass spectrum of the protonated molecule of the octaethoxylate of tetramethyldecyne diol (Surfynol 465, Table 1), $m/z = 579$. The actual structures of components (sites of chain-branching and hydrophile distribution) in this sample mixture are unknown. The charge-initiated C pathway leads to protonated PEG molecules at $m/z = 371, 327, 283, 239, 195$, and 151 ($n = 8$ through $n = 3$). The series commences with loss of the hydroxy-substituted, unsaturated hydrophobe as the alkene, $C_{14}H_{24}O$, 208 u. Members of the series are much more abundant than was found for the secondary or branched alcohol ethoxylates (Figures 3 and 4). This may be due to the probability that both hydroxyl groups are ethoxylated and the parent ion is composed of a mixture of isomers of different ethoxylate lengths. The ion at $m/z = 191$ appears unique to

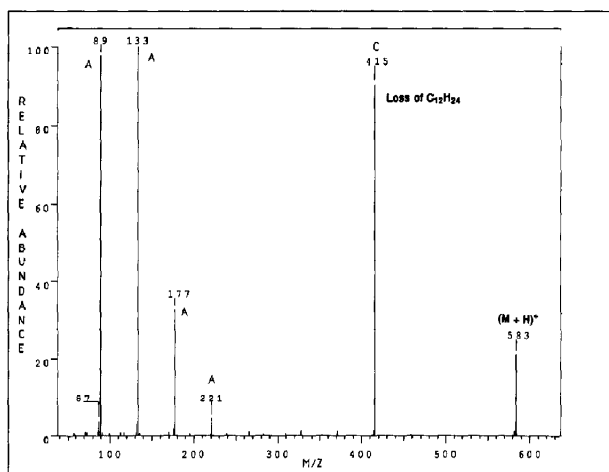
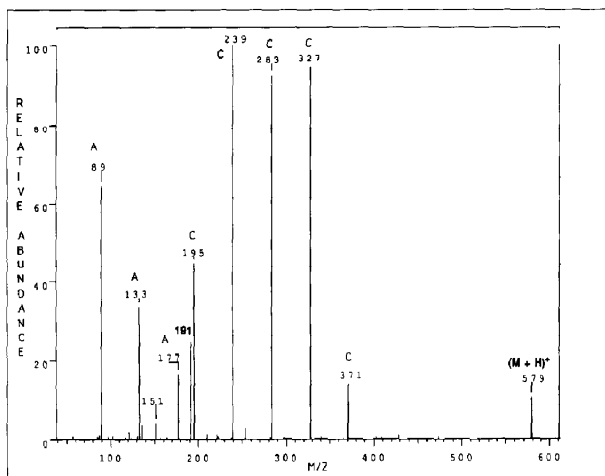


Figure 4. The 40-eV argon CID mass spectrum of the protonated molecule of trimethylnonyl nonaethoxylate, $m/z = 583$, from Tergitol TMN-6. A sample mixture of this branched alcohol ethoxylate was separated using carbon dioxide SFC prior to isobutane (3 torr) PCI, as described in Experimental. The fragment ion mass range was scanned from 50 to 625 u.

Figure 5. The 40-eV argon CID mass spectrum of the protonated molecule of the octaethoxylate of tetramethylethylenediol, $m/z = 579$, from Surfynol 465. Supercritical carbon dioxide was used for sample separation prior to isobutane (3 torr) CI. The fragment ion mass range was scanned from 50 to 650 u.



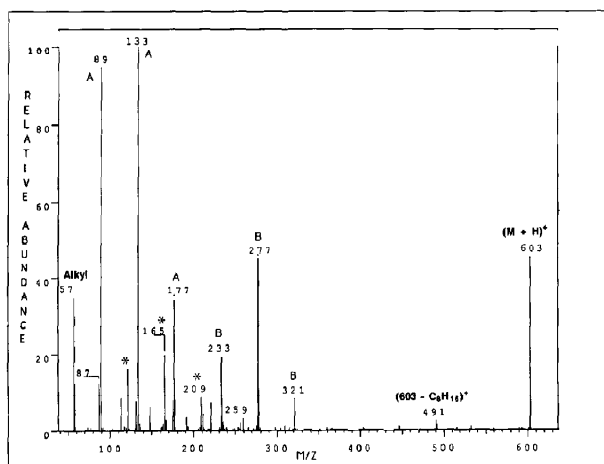
this sample and nominally corresponds to $C_{14}H_{23}^+$. Complete loss of the ethoxylation from both sides of the parent ions and one hydrogen would account for the formation of the m/z 191 ion. A small ion signal is found at m/z 135, corresponding to a loss of 56 u, C_4H_8 , from the m/z 191 species. The $(M + NH_4)^+$ ion, produced in ammonia PCI, showed greater stability to CID than did the protonated molecule and did not exhibit an ion corresponding to loss of ammonia, NH_3 . These details suggest the site of ionization may be different for this material than for the hydrocarbon alcohol ethoxylates. The triple bond may also play some role in the fragmentation. Unfortunately, the CID spectra are most strongly characterized by fragmentations found for saturated hydrocarbon hydrophobes and there appears to be insufficient infor-

mation for complete characterization of hydrophobe structure.

The C pathway is unavailable to alkylphenol ethoxylate ions and Figure 6 shows A and B ions characterize the 40-eV argon CID mass spectrum of octylphenol nonaethoxylate (Triton X-165, Table 1) protonated molecule, $m/z = 603$. Protonated molecules could be produced for this sample, even in ammonia chemical ionization. B ions correspond to octylphenol with one ($m/z = 233$), two ($m/z = 277$), and three ($m/z = 321$) molecules of ethylene glycol, supporting an ionization site close to the hydrophobe.

The octylphenol cation is not found, but many ions due to fragmentation of the hydrophobe are present. The high proton affinity of the ethoxylate chain suggests that fragments are formed remote from the

Figure 6. The 40-eV argon CID mass spectrum of the protonated molecule of octylphenol nonaethoxylate, $m/z = 603$, from Triton X-165. Supercritical carbon dioxide was used for capillary chromatographic separation of the sample mixture and ammonia (7 torr) used for PCI. Ions marked * at $m/z = 121$, 165, and 209 correspond to benzene with one, two, and three ethylene oxide units. The fragment ion mass range was scanned from 50 to 625 u.

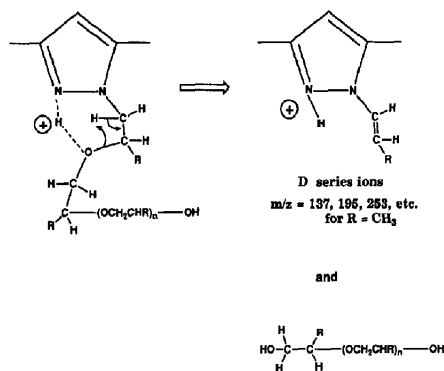


charge site [16, 17]. The first hydrophobe fragment ion, $m/z = 491$, corresponds to loss of octene, 112 u, from the protonated molecule. Ions marked with an asterisk (*, $m/z = 121, 165, \text{ and } 209$) correspond to ethoxylated benzene, analogous to the ions at $m/z = 233, 277, \text{ and } 321$. Relative abundances of the lower molecular weight series resemble those of the higher molecular weight ions. The ion at $m/z = 113$ corresponds to an octyl cation and the $m/z = 57$ species to a butyl cation. Direct loss of the butyl group, with charge retention on the ethoxylated molecule, is not seen.

Loss of *t*-butyl from the alkyl group and lack of C series ions appear characteristic for alkylphenol alkoxylates. Such characteristics are useful in assisting structural identification of these materials in "unknown" mixtures. Unlike other nonionic surfactants, no ions indicative of the complete hydrophobe or hydrophile are produced.

Influence of the hydrophobe or terminal group is even more pronounced when the group is capable of providing a site for charge localization. The 60-eV (lab) argon CID mass spectrum of pyrazole octapropoxylate from Oxypruf "P" ($m/z = 561$) is shown in Figure 7. Only protonated molecules are formed for the propoxylated and ethoxylated versions of this material, regardless of CI reagent. The protonated molecules are also very stable to low energy CID (40-100 eV, lab) with little loss of parent ion current even at high collision energies (100 eV). A single A series ion is found at $m/z = 59$ with all other ions from one series composed of the pyrazole ring, a propylene group and increasing numbers of propylene oxide units. The same characteristics are found for CID mass spectra of the ethoxylated material.

The ion series found for the Oxypruf materials ($m/z = 137, 195, 253, \text{ etc.}$) may be explained by a



Scheme III. A mechanism to explain the fragment ions observed in the low energy CID of alkoxylated pyrazole protonated molecules. This route is a variation of the ether cleavage mechanism illustrated in Scheme II. The alkoxylate chain may coil around to solvate the proton on the pyrazole ring and lead to loss of most of the alkoxylate chain as an alcohol.

version of the charge site-initiated mechanism in Scheme II. The alkoxylate chain may coil or wrap around to solvate the proton on the pyrazole ring, with a hydrogen bond formed with the ether oxygen. This is detailed in the mechanism shown in Scheme III. The ether oxygens nearest the ring are most likely, sterically, to solvate the proton, favoring loss of most of the alkoxylate chain. This may help explain the preference for fragment ions with few alkylene oxide units. In contrast to other alkoxylated surfactants studied, alkoxylated pyrazoles do not solvate ammonia and the protonated molecules are highly resistant to CID. Other decomposition mechanisms can be conceived to explain the differences between

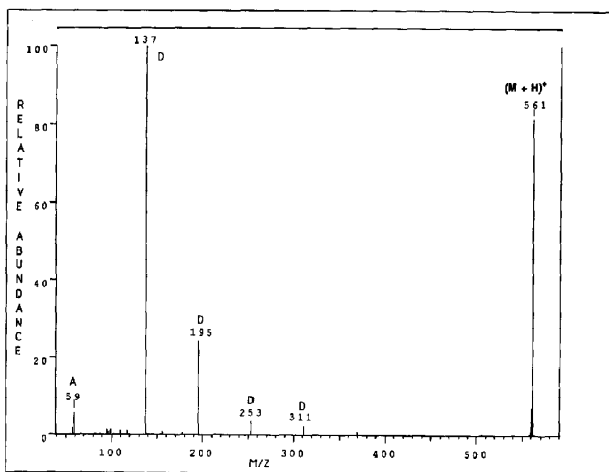


Figure 7. The 60-eV argon CID mass spectrum of the protonated molecule of pyrazole octapropoxylate, $m/z = 561$, from Oxypruf "P". Capillary SFC separation of the sample mixture was performed using carbon dioxide with isobutane (3 torr) used for PCI. Relative abundances for ions from $m/z = 240$ to $m/z = 400$ have been multiplied by a factor of 25. The fragment ion mass range was scanned from 50 to 580 u.

the alkoxyated pyrazoles and other alkoxyated surfactants. The actual decomposition mechanism for alkoxyated pyrazoles may be some combination of fragmentations and further studies are underway to clarify this point.

Conclusions

Capillary SFC combined with CI quadrupole MS/MS provides a rapid and direct method for structural characterization of nonionic surfactant mixtures. The approach also provides a means to probe the mechanisms involved in CID of alkoxyated ions produced using CI. The mobile phase used for SFC separation/introduction does not interfere with CID studies and can be used as the CI reagent for additional information or flexibility. The mechanisms involved in CID of CI-produced nonionic surfactant ions consist mainly of charge site-initiated cleavages and ether linkage cleavages with hydrogen transposition. Fragment ions displayed by the various nonionic surfactant types studied indicate the hydrophobe plays a strong role in determining which mechanisms dominate the low energy CID mass spectrum. This leads to production of diagnostic ions for the various hydrophobe types, such as alkene loss ions, benzene ethoxylate ions, and protonated PEG molecules, key in the overall characterization of components in complex nonionic surfactant mixtures. Although the alkoxyate chain appears to be the site of protonation for nonionic surfactant materials, extensive fragmentation can occur on the hydrophobe chain. Depending on hydrophobe type, further information on the hydrophobe structure may be available from these low molecular weight ions. Diagnostic ions can also be used to determine length of hydrophobe and hydrophile chains.

The study illustrates a weakness in CI followed by low energy CID for characterization of highly functionalized molecules, the inability to differentiate isomeric forms of the hydrophobe. It may be necessary to use a more energetic ionization method, charge-exchange CI with supercritical fluid injection for example, to produce hydrophobe-specific ions for further structural characterization by CID. It may be necessary to use high energy collisions to produce fragment information regarding the hydrophobe. Work is underway to explore some of these approaches.

The present study provides a comprehensive comparison of the types of CID daughter ions formed from a wide variety of nonionic surfactant materials. The efforts form a baseline for further comparison of introduction techniques for CID MS/MS of surfactants and the wide range of other materials amenable to supercritical fluid solvation. The distinctions in mechanisms in high and low energy MS/MS may also be probed using supercritical fluid introduction.

References

1. Kalinoski, H. T.; Hargiss, L. O. *J. Chromatogr.* **1989**, *474*, 69-82.
2. Pinkston, J. D.; Bowling, D. J.; Delaney, T. E. *J. Chromatogr.* **1989**, *474*, 97-111.
3. Kalinoski, H. T.; Hargiss, L. O. *J. Chromatogr.* **1990**, *505*, 199-213.
4. Smith, R. D.; Kalinoski, H. T.; Udseth, H. R. *Mass Spectrom. Rev.* **1987**, *6*, 445-496.
5. Chester, T. L.; Pinkston, J. D. *Anal. Chem.* **1990**, *62*, 394R-402R.
6. Owens, G. D.; Burkes, L. J.; Pinkston, J. D.; Keough, T.; Simms, J. R.; Lacey, M. P. In *Supercritical Fluid Extraction and Chromatography*; Charpentier, B. A., Sevenants, M. R., Eds.; ACS Symposium Series 366; American Chemical Society: Washington, DC, 1988; pp 191-207.
7. Baumeister, E. D.; West, C. D.; Ijames, C. F.; Wilkens, C. L. *Anal. Chem.* **1991**, *63*, 251-255.
8. Lattimer, R. P.; Münster, H.; Budzikiewicz, H. *Int. J. Mass Spectrom. Ion Processes* **1989**, *90*, 119-129.
9. Lammert, S. A. Finnigan-MAT Technical Report Number 603, 1987.
10. Kiplinger, J. P.; Bursey, M. M. *Org. Mass Spectrom.* **1988**, *23*, 342-349.
11. Jensen, N.; Musselman, B. D.; Tamura, J. In *Proceedings of the 38th Annual Conference on Mass Spectrometry and Allied Topics*, June 3-8, 1990; pp 876-877.
12. JEOL Application Note—Mass Spectrometry, MS 69, 1990.
13. Lin, H.-Y.; Rockwood, A. L.; Ridge, D. P. In *Proceedings of the 38th Annual Conference on Mass Spectrometry and Allied Topics*, June 3-8, 1990; pp 471-472.
14. Rivera, J.; Ventura, F.; Caixach, J.; Fraisse, D. *Proceedings of the 38th Annual Conference on Mass Spectrometry and Allied Topics*, June 3-8, 1990; pp 655-656.
15. Wysocki, V. H.; Ross, M. M. *Int. J. Mass Spectrom. Ion Processes*, **1991**, *104*, 179-212.
16. Adams, J.; Gross, M. L. *J. Am. Chem. Soc.* **1986**, *108*, 6915-6921.
17. Adams, J. *Mass Spectrom. Rev.* **1990**, 141-186.